

Enhanced Si and B diffusion in semiconductor-grade SiO₂ and the effect of strain on diffusion

Masashi Uematsu ^{a,*}, Hiroyuki Kageshima ^a, Shigeto Fukatsu ^b, Kohei M. Itoh ^b, Kenji Shiraishi ^c, Minoru Otani ^d, Atsushi Oshiyama ^c

^a NTT Basic Research Laboratories, NTT Corporation, 3-1 Morinosato-Wakamiya, Atsugi 243-0198, Japan

^b Keio University and CREST-JST, 3-14-1 Hiyoshi, Kohoku-ku, Yokohama 223-8522, Japan

^c University of Tsukuba, 1-1-1 Tennodai, Tsukuba 305-8571, Japan

^d Institute for Solid State Physics, University of Tokyo, 5-1-5 Kashiwanoha, Kashiwa 277-8581, Japan

Available online 9 November 2005

Abstract

We present experimental and simulation results of Si self-diffusion and B diffusion in SiO₂ formed directly on Si substrates by thermal oxidation. We show that both Si and B diffusion in SiO₂ are enhanced by SiO generated at the Si/SiO₂ interface and diffusing into SiO₂. We also show that the existence of high-concentration B in SiO₂ enhances SiO diffusion, which enhances both Si self-diffusion and B diffusion. This correlated diffusion of Si and B in SiO₂ is consistent with the first-principles calculation results, which show that B diffuses via a complex of BSiO with frequent bond exchanges in the SiO₂ network. Furthermore, based on the results, the enhancement of Si self-diffusion and B diffusion in SiO₂ by compressive strain and their retardation by tensile strain are suggested.

© 2005 Elsevier B.V. All rights reserved.

Keywords: Diffusion; Silicon oxide; Boron; Stress

1. Introduction

Thermally grown SiO₂ on Si substrates is one of the most important heterostructures in Si devices, especially for the gate structure of metal-oxide-semiconductor (MOS) transistors. With the scaling-down of MOS transistors, an ultrathin SiO₂ layer is demanded for the gate insulator. As the thickness of the SiO₂ layer decreases, atomic and molecular diffusion in SiO₂ becomes a fundamental issue. Concerning impurity diffusion, B penetration from the gate electrode through the thin SiO₂ layer into the Si substrate has been recognized as a serious problem [1]. The diffusion in SiO₂ is also an important issue in high-k gate dielectrics because an interfacial SiO₂ layer forms between high-k gate films and Si substrates during post-annealing [2]. In addition, diffusion in SiO₂ is closely related to the viscosity of SiO₂, which is an important property of materials, and compressive strain in SiO₂ results in higher rate constants for atomic transport processes such as diffusion and

viscous flow [3,4]. The present work investigates Si self-diffusion and B diffusion in SiO₂ formed directly on Si substrates by thermal oxidation. We show that Si and B diffusion in SiO₂ is enhanced by SiO generated at the Si/SiO₂ interface and diffusing into SiO₂ and that SiO diffusion is enhanced by the existence of high-concentration B. This correlated diffusion of Si and B in SiO₂ is supported by the first-principles calculation, which shows that SiO diffuses via frequent atomic exchanges with substitutional atoms. Furthermore, based on the results, the effect of strain on the diffusion in SiO₂ is discussed.

2. Enhanced Si and B diffusion

An isotopically enriched ²⁸Si single crystal epi-layer was thermally oxidized in dry O₂ at 1100 °C to form ²⁸SiO₂ of thicknesses of 200, 300, and 650 nm. The samples were implanted with ³⁰Si at 50 keV to a dose of 2×10^{15} cm⁻² and capped with a 30 nm thick silicon nitride layer. Subsequently, the samples were implanted with ¹¹B at 25 keV to a dose of 5×10^{13} or 3×10^{15} cm⁻², which will be referred to as low-dose and high-dose samples, respectively. In some samples, B

* Corresponding author. Tel.: +81 46 240 2883; fax: +81 46 240 4317.

E-mail address: uematsu@aecl.nnt.co.jp (M. Uematsu).

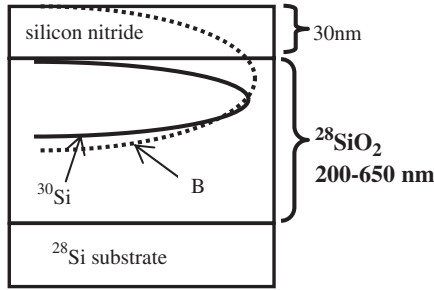


Fig. 1. The sample structure.

implantation was not performed. The sample structure is shown in Fig. 1. Samples were pre-annealed at 1000 °C for 30 min to eliminate implantation damage and diffusion-annealed at temperatures between 1100 and 1250 °C. The depth profiles of ³⁰Si and B were measured by secondary ion mass spectrometry (SIMS).

The experimental ³⁰Si depth profiles in the samples without B implantation after annealing for 24 h at 1250 °C are shown in Fig. 2. The samples demonstrate a strong dependence on the thickness of the ²⁸SiO₂ layer; the thinner the ²⁸SiO₂ layer is, the broader the diffusion profile becomes [5,6]. This result shows that the Si self-diffusivity increases with decreasing distance between the diffusing ³⁰Si species and ²⁸Si/²⁸SiO₂ interface. This dependence on the distance from the Si/SiO₂ interface was also observed for B diffusion in SiO₂. Fig. 3 shows the experimental B profiles in low-dose samples after annealing at

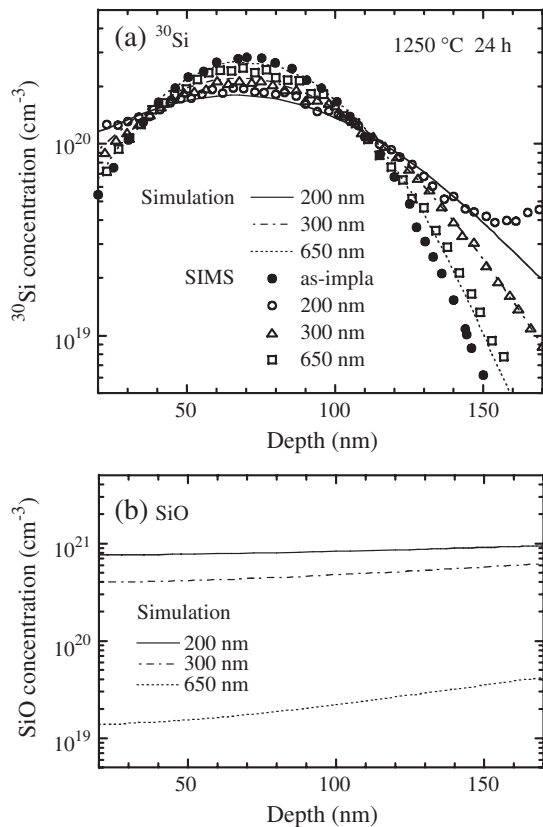


Fig. 2. (a) Experimental and simulated ³⁰Si depth profiles, and (b) simulated SiO profiles in SiO₂ samples without B implantation. Samples were annealed at 1250 °C for 24 h.

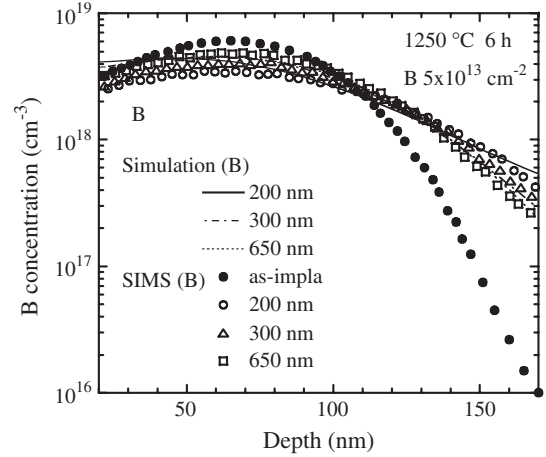
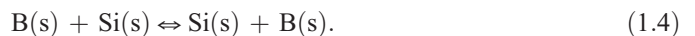
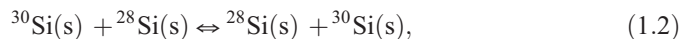


Fig. 3. Experimental and simulated B depth profiles in SiO₂ samples. Samples were implanted with B to a dose of $5 \times 10^{13} \text{ cm}^{-2}$ (low B dose) and annealed at 1250 °C for 6 h.

1250 °C for 6 h. In the same way as Si self-diffusion, the B diffusion demonstrates a clear dependence on the thickness of the ²⁸SiO₂ layer; the shorter the distance from the Si/SiO₂ interface, the higher the B diffusivity in SiO₂ [7,8]. This tendency was observed consistently in Si and B diffusion for other temperatures and annealing times employed in this study.

As a possible origin of the distance dependence of Si and B diffusion, we examined the effect of implantation damage; however, we found that it is of no concern because the self-diffusivity of implanted Si in thick SiO₂ agrees with that obtained from damage-free CVD (chemical vapor deposition) SiO₂ [9] and remains unchanged for the doses between 1×10^{14} and $2 \times 10^{15} \text{ cm}^{-2}$. In addition, we have performed an experiment using CVD isotope heterostructures with a constant total oxide thickness and found that the Si self-diffusivity increases with decreasing the distance from the interface in the same way as that described above [10]. These results lead us to conclude that Si species generated at the Si/SiO₂ interface and diffusing into SiO₂ enhance both Si and B diffusion. There have been a number of suggestions, based on experimental speculations and theoretical predictions, regarding the emission of Si species from the Si/SiO₂ interface to SiO₂ [11–13], and SiO generated at the Si/SiO₂ interface via the reaction $\text{Si} + \text{SiO}_2 \rightarrow 2\text{SiO}$ is the most likely candidate as the dominant Si species. Consequently, we have proposed a model where SiO generated at the Si/SiO₂ interface and diffusing into SiO₂ enhances both Si self-diffusion and B diffusion in SiO₂ via the reaction



In these equations, Si and B atoms substituted in the Si sites of SiO₂ [denoted as (s)] diffuse via the kick-out reaction with

diffusing SiO. In addition, a simple mechanism of Si self-diffusion and B diffusion, where SiO is not involved, is taken into account for the thermal Si self-diffusion and B diffusion, as described by Eqs. (1.2) and (1.4). Evidence for the existence of two mechanisms (with and without SiO) is that very little SiO arrive from the interface in the 650 nm thick sample, as will be shown later by the simulation. B diffusion via SiO [Eq. (1.3)] is similar to B diffusion in Si via the kick-out mechanism, and BO may correspond to a complex of BSiO according to the first-principle calculation of B diffusion in SiO₂ [14,15].

The above model leads to the following set of coupled partial differential equations to describe the diffusion of ³⁰Si and B in ²⁸SiO₂:

$$\frac{\partial C_{30\text{Si}}}{\partial t} = \frac{\partial}{\partial x} \left(D_{\text{Si}}^{\text{SD(th)}} \frac{\partial C_{30\text{Si}}}{\partial x} \right) - R_1, \quad (2.1)$$

$$\frac{\partial C_{30\text{SiO}}}{\partial t} = \frac{\partial}{\partial x} \left(D_{\text{SiO}} \frac{\partial C_{30\text{SiO}}}{\partial x} \right) + R_1, \quad (2.2)$$

$$\frac{\partial C_{28\text{SiO}}}{\partial t} = \frac{\partial}{\partial x} \left(D_{\text{SiO}} \frac{\partial C_{28\text{SiO}}}{\partial x} \right) - R_1 - R_2, \quad (2.3)$$

$$\frac{\partial C_{\text{B}}}{\partial t} = \frac{\partial}{\partial x} \left(D_{\text{B}}^{\text{eff(th)}} \frac{\partial C_{\text{B}}}{\partial x} \right) - R_2, \quad (2.4)$$

$$\frac{\partial C_{\text{BO}}}{\partial t} = \frac{\partial}{\partial x} \left(D_{\text{BO}} \frac{\partial C_{\text{BO}}}{\partial x} \right) + R_2, \quad (2.5)$$

where R_1 and R_2 are the reaction terms for Eqs. (1.1) and (1.3), respectively, and described by

$$R_1 = k_{f1} C_{30\text{Si}} C_{28\text{SiO}} - k_{b1} C_{30\text{SiO}}, \quad (3.1)$$

$$R_2 = k_{f2} C_{\text{B}} C_{28\text{SiO}} - k_{b2} C_{\text{BO}}. \quad (3.2)$$

The Si self-diffusivity and the effective B diffusivity are, as a whole, described by

$$D_{\text{Si}}^{\text{SD}} = D_{\text{Si}}^{\text{SD(th)}} + D_{\text{SiO}}^{\text{SD}} \frac{C_{28\text{SiO}}(x, t)}{C_{\text{SiO}}^{\text{max}}}, \quad (4.1)$$

$$D_{\text{B}}^{\text{eff}} = D_{\text{B}}^{\text{eff(th)}} + D_{\text{i}}^{\text{eff}} \frac{C_{28\text{SiO}}(x, t)}{C_{\text{SiO}}^{\text{max}}}. \quad (4.2)$$

In these equations, C_x is the concentration of the corresponding species in Eqs. (1.1)–(1.4), $D_{\text{Si}}^{\text{SD(th)}}$ the thermal Si self-diffusivity, D_{SiO} the diffusivity of SiO, $D_{\text{B}}^{\text{eff(th)}}$ the effective diffusivity of thermal B diffusion, D_{BO} the diffusivity of BO, and k_f and k_b are the forward and backward rate constants of Eqs. (1.1) and (1.3). In Eq. (2.1), the thermal Si self-diffusion [Eq. (1.2)] is represented by the diffusion term with $D_{\text{Si}}^{\text{SD(th)}}$, and $D_{\text{Si}}^{\text{SD(th)}} = 0.8 \exp(-5.2 \text{ eV/kT}) \text{ cm}^2/\text{s}$ [9] that was experimentally obtained is used for the simulation. Similarly, the thermal B diffusion [Eq. (1.4)] is represented by the diffusion term with $D_{\text{B}}^{\text{eff(th)}}$ in Eq. (2.4), and the experimentally obtained B diffusivity in thick ($>1 \mu\text{m}$) SiO₂,

$D_{\text{B}}^{\text{eff(th)}} = 3.12 \times 10^{-3} \exp(-3.93 \text{ eV/kT}) \text{ cm}^2/\text{s}$ [16], is used. In Eq. (4.1), $D_{\text{SiO}}^{\text{SD}} = D_{\text{SiO}} C_{\text{SiO}}^{\text{max}}/N_0$ is the Si self-diffusivity via SiO, where N_0 denotes the number of SiO₂ molecules in a unit volume of silicon oxide. Here, $C_{\text{SiO}}^{\text{max}}$ denotes the maximum SiO concentration in SiO₂ and is described as $C_{\text{SiO}}^{\text{max}} = 3.6 \times 10^{24} \exp(-1.07 \text{ eV/kT}) \text{ cm}^{-3}$ [6]. In Eq. (4.2), $D_{\text{i}}^{\text{eff}} = D_{\text{BO}} C_{\text{BO}}^{\text{eq}}/C_{\text{B}}$ is the effective diffusivity of B diffusion via the kick-out mechanism with SiO ($C_{\text{BO}}^{\text{eq}}$ is the equilibrium concentration of BO). In Eqs. (4.1) and (4.2), $C_{28\text{SiO}}(x, t)$ depends on the depth and annealing times, which will be described below. The ²⁸SiO concentration at the ²⁸Si/²⁸SiO₂ interface is fixed at $C_{\text{SiO}}^{\text{max}}$ to describe the generation of SiO at the interface. Reactions (1.1)–(1.4) are assumed to be so fast that the local equilibrium of the reaction is established, and hence the rate constants are set to be large enough. The parameters deduced from the simulation to fit the experimental profiles of ³⁰Si and B are $D_{\text{SiO}}^{\text{SD}}$ and $D_{\text{i}}^{\text{eff}}$, and we consistently obtained $D_{\text{SiO}}^{\text{SD}} = 4 \times 10^4 \exp(-6.2 \text{ eV/kT}) \text{ cm}^2/\text{s}$ and $D_{\text{i}}^{\text{eff}} = 6.4 \times 10^{-2} \exp(-4.1 \text{ eV/kT}) \text{ cm}^2/\text{s}$ for all samples. Eqs. (2.1)–(2.5) were solved numerically by the partial differential equation solver ZOMBIE [17].

Figs. 2 and 3 show the simulated depth profiles of ³⁰Si and B, respectively, after annealing at 1250 °C. For the simulated ³⁰Si profiles, the concentration of ³⁰Si(s) is shown because it is about two orders of magnitude larger than that of ³⁰SiO. The simulation results fit the experimental profiles of ³⁰Si and B for all ²⁸SiO₂ thicknesses using the same parameter values. In Fig. 2(b), the simulated ²⁸SiO profiles are also shown and the SiO concentration in the region of ³⁰Si and B increases with decreasing ²⁸SiO₂ thickness. As expected from Eqs. (4.1) and (4.2), SiO with higher concentration leads to larger enhancement of ³⁰Si and B diffusion. Therefore, Si self-diffusion and B diffusion become faster with decreasing ²⁸SiO₂ thickness. This thickness dependence arises because the SiO diffusion is so slow that the SiO concentration critically depends on the distance from the Si/SiO₂ interface, where the SiO is generated. In addition, the profile of SiO for the 650 nm thick sample shows that the SiO concentration is so small that Si and B diffusion cannot be explained only by the kick-out diffusion via SiO [Eqs. (1.1)–(1.4)]. This is the evidence for the existence of the two mechanisms (with and without SiO), as described above. We mention that the simulation predicts the possibility of time-dependent diffusivities for Si and B because more SiO should be arriving from the interface with time, and this time dependence was experimentally observed.

3. Enhancement by high-concentration B

Fig. 4 shows the depth profiles of ³⁰Si and B in the high-dose 200 nm thick sample after diffusion anneal of 6 h at 1250 °C. The ³⁰Si depth profile of the annealed sample without B implantation is also shown. The profile of ³⁰Si in the high-dose samples shows larger diffusion than that without B [7,8]. On the other hand, the ³⁰Si profile of the low-dose samples (not shown in Fig. 4) showed no significant difference from that without B. In addition, for the high-dose sample, a significant decrease in the ³⁰Si concentration at its peak region was

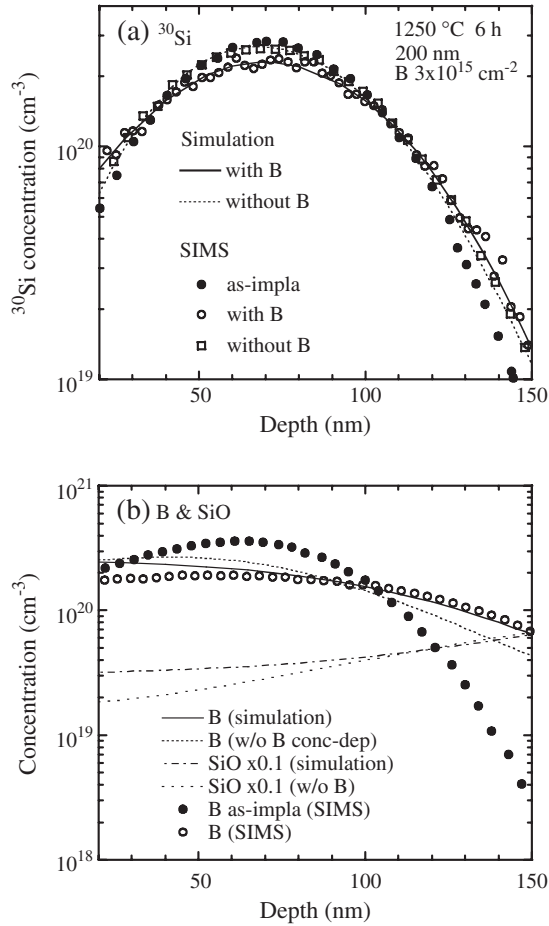


Fig. 4. (a) Experimental and simulated ^{30}Si depth profiles with high-dose B implantation ($3 \times 10^{15} \text{ cm}^{-2}$) and without B, and (b) experimental and simulated B depth profiles and the simulated SiO profile (multiplied by 0.1) with high B dose in the 200 nm thick sample after annealing for 6 h at 1250 °C. In (b), the result of simulation without B concentration dependence and the simulated SiO profile (multiplied by 0.1) without B are also shown.

observed, where B concentration is high. In contrast, the tail region of ^{30}Si showed less significant diffusion, where B concentration is low. These results show that Si self-diffusivity increases with higher B concentration in SiO_2 . This dependence of B concentration is also seen in B diffusion itself. Fig. 4(b) compares the experimental and simulated B profiles in the 200 nm thick sample with high B dose after annealing at 1250 °C for 6 h. With the D_i^{eff} given above, the B diffusion profiles of low-dose samples were well reproduced by the simulation, as described in the previous section. However, the same simulation of the B diffusion for high-dose samples underestimated the results, as shown by the dotted line. This result shows that B diffusion in high-dose samples is faster than that in low-dose samples and that B diffusivity also increases with higher B concentration. The B concentration dependence has been reported in an experiment using a MOS structure, where the B diffusivity abruptly increased above B concentration of 10^{20} cm^{-3} [18], which is consistent with our result.

In order to reproduce the experimentally obtained enhancement of the ^{30}Si and B diffusion in the high-dose sample, we introduced a B concentration dependence of $D_{\text{SiO}}^{\text{SD}}$ and D_i^{eff} for

Si self-diffusion and B diffusion via SiO, of $D_{\text{Si}}^{\text{SD(th)}}$ for thermal Si self-diffusion, and of $D_{\text{B}}^{\text{eff(th)}}$ for thermal B diffusion by multiplying a factor of $\exp(C_{\text{B}}/C_{\text{B}}^{\text{cri}})$ to imitate the strong dependence on B concentration, where $C_{\text{B}}^{\text{cri}}$ denotes the critical B concentration above which the high-concentration effect occurs. Inclusion of the B concentration dependence [$\times \exp(C_{\text{B}}/C_{\text{B}}^{\text{cri}})$] of $D_{\text{Si}}^{\text{SD(th)}}$ and $D_{\text{B}}^{\text{eff(th)}}$ is essential for explaining the enhancement of Si self-diffusion and B diffusion in the 650 nm thick sample, where very little SiO arrive from the interface. Consequently, the factor $\exp(C_{\text{B}}/C_{\text{B}}^{\text{cri}})$ was applied to $D_{\text{Si}}^{\text{SD}}$ and $D_{\text{B}}^{\text{eff}}$ [Eqs. (4.1) and (4.2)], which represent the sum of the two contributions (thermal diffusion and diffusion via SiO) to Si self-diffusion and B diffusion. Using the value of $C_{\text{B}}^{\text{cri}} = 2 \times 10^{20} \text{ cm}^{-3}$, ^{30}Si and B profiles in the high-B-dose samples were fitted by the same set of diffusion parameters as that for low-dose profiles and that without B, as shown in Fig. 4. The profiles of SiO (multiplied by 0.1) obtained from the simulation are also shown in Fig. 4(b). In the near-surface region, the SiO concentration with high B dose is higher than that without B because the SiO diffusivity is enhanced by the B concentration dependence, which leads to the increase of Si self-diffusivity and B diffusivity with higher B concentration. The present result indicates that Si and B atoms in SiO_2 diffuse correlatively via SiO; namely, the enhanced SiO diffusion caused by the existence of B enhances B diffusion and Si self-diffusion. This correlation is consistent with the first-principles calculation of B diffusion in SiO_2 , as described below. In addition, the present results explain why the incorporation of B in SiO_2 reduces the viscosity of SiO_2 , which is inversely proportional to SiO diffusivity [19].

4. Effect of strain on diffusion

In order to investigate the effect of strain on diffusion in SiO_2 , it is necessary to examine the microscopic mechanism of the diffusion. Fig. 5 shows the geometries during B diffusion obtained from the first-principles calculation using a supercell containing 72 atoms in α -quartz as a representative of SiO_2 [20]. The calculation results for the +1 charge state are shown in Fig. 5 because this state is the most energetically stable [15]. The details of the calculation are described in Refs. [14,15]. The geometry shown in Fig. 5(a) is the most stable structure because the B–O bond is strong, where the B atom is threefold coordinated with three nearby O atoms, and this geometry corresponds to BO in Eq. (1.3). The most remarkable feature of this geometry is that one of the three O atoms is threefold coordinated. This three-coordinate O atom is formed because the B atom in the SiO_2 network is close enough to the O atom to form a bond. In addition, the B atom remains three-coordinate during the diffusion, as shown below. Starting with this geometry, a variety of possible diffusion pathways toward the final geometry was explored. The results show that the B atom diffuses along bond networks of SiO_2 by breaking and forming bond configurations. Some geometries during the diffusion are shown in Fig. 5. After several breaking and forming of B–O and Si–O bonds, we have the geometry of

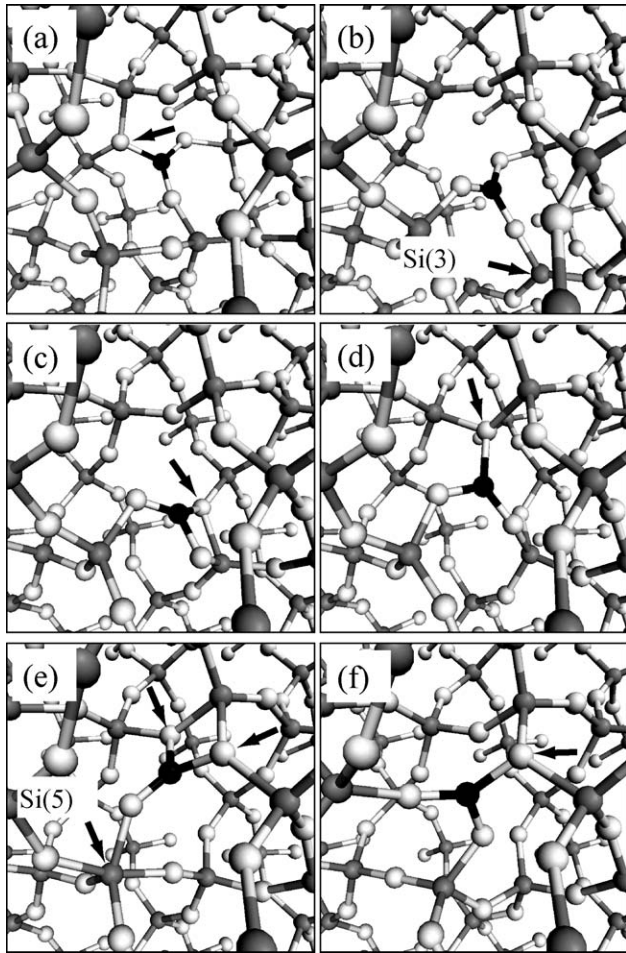


Fig. 5. Change in the geometry during B diffusion in SiO₂. Black, gray, and white balls indicate B, Si, and O atoms, respectively. Arrows indicate three-coordinate O atoms, and S(3) and S(5) indicate three- and five-coordinate Si atoms, respectively.

Fig. 5(b), which has a three-coordinate Si atom and no three-coordinate O atoms. In Fig. 5(c), a three-coordinate O atom is formed again and the three-coordinate Si atom returns to four-coordinate, followed by a change of bonds between the B atom and three-coordinate O atoms [Fig. 5(d)]. With some bond exchanges and network deformations, the saddle point geometry is reached, where one five-coordinated Si atom and two three-coordinate O atoms are involved [Fig. 5(e)]. Then, this geometry returns to a structure with one three-coordinate O atom [Fig. 5(f)]. These changes in geometry show that B diffuses by forming a complex of BSiO with frequent bond exchanges in the SiO₂ network. Note that B and Si atoms in this complex are not the same B and Si atoms in the diffusion process, and different B and Si atoms are involved in atomic exchanges.

The above results provide insight into the effect of strain on diffusion in SiO₂. The geometry change described above indicates that SiO diffuses via the bond exchanges with Si and O atoms of SiO₂, that is, via the reconstruction of Si–O bonds, not via the interstitial mechanism through the open spaces of SiO₂. The increase in pressure makes Si and O atoms closer to each other in SiO₂, and hence enhances the rebonding of Si–O

bonds with other atoms [3,4]. This enhancement should result in higher SiO diffusivity in SiO₂ because SiO diffuses via bond exchanges with Si and O atoms of SiO₂, as discussed above. The same argument holds for B diffusion because the increase in pressure makes B and O atoms closer to each other, and hence enhances the rebonding of B–O and Si–O bonds. As shown above, both Si self-diffusion and B diffusion are enhanced by SiO and in addition B diffuses via BO in SiO₂. Therefore, compressive strain is thought to enhance Si self-diffusion and B diffusion in SiO₂, while tensile strain is thought to retard these diffusions, contrary to the effect expected from the interstitial mechanism. This discussion is supported by what is known about the Si oxidation rate and the viscosity of SiO₂. The simulation of Si nanostructure oxidation indicates that the viscosity of SiO₂ is reduced by the oxidation-induced compressive strain and the diffusion of O₂ molecules in SiO₂ is retarded [21]. The reduction of SiO₂ viscosity is consistent with the enhancement of SiO diffusion by compressive strain. In addition, because O₂ diffuses via interstitial sites through the open spaces of SiO₂ [22,23], the retardation of O₂ diffusion is also consistent with the above discussion.

5. Summary

We have described experimental and simulation results of Si self-diffusion and B diffusion in SiO₂. We showed that both Si self-diffusion and B diffusion are enhanced by SiO. In addition, the results of the B concentration dependence indicate that Si and B atoms in SiO₂ diffuse correlatively via SiO; namely, the enhanced SiO diffusion by the existence of B enhances both Si self-diffusion and B diffusion. This correlated diffusion of Si and B in SiO₂ is supported by the first-principles calculation, which shows that B diffuses via the complex of BSiO with frequent bond exchanges in the SiO₂ network. In addition, the enhancement of Si self-diffusion and B diffusion in SiO₂ by compressive strain and their retardation by tensile strain are suggested.

References

- [1] J.R. Pfeister, L.C. Parrollo, F.K. Baker, IEEE Electron Device Lett. 11 (1990) 247.
- [2] G.D. Wilk, R.M. Wallace, J.M. Anthony, J. Appl. Phys. 89 (2001) 5243.
- [3] S. Tsuneyuki, Y. Matsui, Phys. Rev. Lett. 74 (1995) 3197.
- [4] M.J. Aziz, S. Circone, C.B. Agee, Nature 390 (1997) 596.
- [5] S. Fukatsu, T. Takahashi, K.M. Itoh, M. Uematsu, A. Fujiwara, H. Kageshima, Y. Takahashi, K. Shiraishi, U. Gösele, Appl. Phys. Lett. 83 (2003) 3897.
- [6] M. Uematsu, H. Kageshima, Y. Takahashi, S. Fukatsu, K.M. Itoh, K. Shiraishi, U. Gösele, Appl. Phys. Lett. 84 (2004) 876.
- [7] M. Uematsu, H. Kageshima, Y. Takahashi, S. Fukatsu, K.M. Itoh, K. Shiraishi, Appl. Phys. Lett. 85 (2004) 221.
- [8] M. Uematsu, H. Kageshima, Y. Takahashi, S. Fukatsu, K.M. Itoh, K. Shiraishi, J. Appl. Phys. 96 (2004) 5513.
- [9] T. Takahashi, S. Fukatsu, K.M. Itoh, M. Uematsu, A. Fujiwara, H. Kageshima, Y. Takahashi, K. Shiraishi, J. Appl. Phys. 93 (2003) 3674.
- [10] S. Fukatsu, K.M. Itoh, M. Uematsu, H. Kageshima, Y. Takahashi, K. Shiraishi, Jpn. J. Appl. Phys. 43 (2004) 7837.
- [11] T.Y. Tan, U. Gösele, Appl. Phys. Lett. 40 (1982) 616.
- [12] G.K. Celler, L.E. Trimble, Appl. Phys. Lett. 54 (1989) 1427.

- [13] Y. Takakuwa, M. Nihei, N. Miyamoto, *Appl. Surf. Sci.* 117/118 (1997) 141.
- [14] M. Otani, K. Shiraishi, A. Oshiyama, *Phys. Rev. Lett.* 90 (2003) 075901.
- [15] M. Otani, K. Shiraishi, A. Oshiyama, *Phys. Rev., B* 68 (2003) 184112.
- [16] T. Aoyama, H. Tashiro, K. Suzuki, *J. Electrochem. Soc.* 146 (1999) 1879.
- [17] W. Jüngling, P. Pichler, S. Selberherr, E. Guerrero, H.W. Pötzl, *IEEE Trans. Electron Devices* 32 (1985) 156.
- [18] T. Aoyama, H. Arimoto, K. Horiuchi, *Jpn. J. Appl. Phys.* 40 (2001) 2685.
- [19] R.H. Doremus, *J. Appl. Phys.* 92 (2002) 7619.
- [20] M. Otani, K. Shiraishi, A. Oshiyama, unpublished.
- [21] M. Uematsu, H. Kageshima, K. Shiraishi, M. Nagase, S. Horiguchi, Y. Takahashi, *Solid-State Electron.* 48 (2004) 1073.
- [22] T. Bakos, S.N. Rashkeev, S.T. Pantelides, *Phys. Rev. Lett.* 88 (2002) 055508.
- [23] T. Akiyama, H. Kageshima, T. Ito, *Jpn. J. Appl. Phys.* 43 (2004) 7903.